https://www.sciencedirect.com/science/article/pii/S0009261410004604

Photo-catalytic oxidation reaction of gaseous mercury over titanium dioxide nanoparticle surfaces

Graydon Snider, Parisa Ariya

Abstract

$Hg^0(g)$ is known to undergo photo-catalytic oxidation by UVA-irradiated TiO_2 surfaces. One micrometre layers of TiO_2 on quartz glass were irradiated within the 240–800 nm range. Gaseous mercury was measured by mass spectrometry single ion monitoring. The surface configuration and elemental characterization of TiO_2 layer was evaluated using scanning electron microcopy with energy dispersive spectroscopy. The LH adsorption constant of was found to be $K_{Hg} = (5.1 \pm 2.4) \times 10^{-14}$ cm^3 and an apparent surface deposition rate of $k = (7.4 \pm 2.5) \times 10^{14}$ min^{-1} cm^{-2} under experimental conditions. Water did not affect the rate constant. We show TiO_2 could be employed to reduce mercury concentrations in gas streams, even at very high Hg^0 concentrations.

1. Introduction

Mercury is a neurotoxic heavy metal [1] released anthropogenically from coal combustion and trash incineration [2]. For in- stance, nearly half of all power in the United States is derived from coal [3]. The only long-term solutions for these problems are drastic reductions on our dependence of non-renewable goods and maximizing recycling. The use of coal as an energy source is likely to grow in the coming decade despite research into alternative energy sources [4]. Interim goals are necessary to reduce heavy metal emissions in the atmosphere. In parallel to the numerous proposals for CO_2 reduction through carbon sequestration, removing toxic heavy metals from combustion is an equally open and active area of research [5]. Here we aim to study the capacity of titanium dioxide for removing gaseous mercury from air with a focus on the physical chemistry of surface adsorption, and the effects of water on uptake efficiency.

Gaseous mercury, $Hg^0(g)$, has a long atmospheric lifetime of 0.5–2 years [6], allowing emissions to disperse globally. Gaseous elemental mercury deposition, both wet and dry, deposits into aquatic ecosystems transformed into methyl mercury by sulfate- reducing bacteria [7]. Methylated mercury can be incorporated and biomagnified through the food chain eventually leading to fish advisories from the increasingly dangerous levels of methyl mercury found in edible fish [7].

Titanium dioxide (TiO_2) is a popular heterogeneous catalyst for hydrocarbon oxidation whose surface properties [8] and photocatalytic potential [9] have been extensively studied. TiO_2 can crystallize into rutile, anatase, or (non-photolytic) brookite structures [10]. A mixture of anatase and rutile TiO_2 are typically found in oxide film coatings [11]. Titanium dioxide is a candidate for scavenging gaseous mercury. It has long been known that TiO_2 powders and films are photolytically active under UVA (320 6 k 6 400 nm) light [11]. Hydrocarbons adsorbed to the surface of TiO_2 are oxidized heterogeneously. Such a system has been used to decompose harmful hydrocarbons and bacteria [8]. Elemental mercury can be similarly oxidized under room temperature conditions in air, to mercury oxide [12,13], which is a non-volatile solid characterized by nano-scale zigzag chains of Hg–O.

The threshold energy required to generate electron–hole pairs (i.e. excite from the valence to conduction band) in titania is 3.2 eV or about 380 nm (UVA light) [14]. The mechanism of photo-catalytic oxidation depends to some extent on the oxidant reaction in question. Here it begins with an adsorbed oxygen molecule that traps the 'free' electron and reducing it to superoxide:

$$O_2 + \acute{e} \rightarrow O_2^{\cdot -} \quad (1)$$

The hole may then oxidize water to the hydroxyl radical

$$H_2O + h^+ \rightarrow OH^{\cdot} + H^+ \quad (2)$$

OH was then assumed to oxidize the adsorbed mercury into HgO(s) [15].

It is assumed that HgO(s) will both decompose into $Hg^0(g)$ above 500 °C [16] and is soluble in nitric acid, whereas TiO_2 melts at 1560 °C and is insoluble in most acids [17]. The proper means for disposing chemisorbed HgO remains to be determined and is a parallel subject of research [18].

A growing body of research is focused on the oxidation of $Hg^0(g)$ by UVA (320–400 nm) irradiated TiO_2 (e.g. Wu et al. [13], Lee et al. [19], Pitoniak et al. [20] and Prairie et al. [21]). For instance, Li and Wu [22,23] oxidized $Hg^0(g)$ using TiO_2–SiO_2 nanocomposites, and Rodríguez et al. [15] oxidized mercury over TiO_2 coated on quartz irradiated at 320 6 k 6 400 nm (UVA). The application of TiO_2 films to mercury oxidation is attractive as it can be performed at room temperature. Several methods require higher temperatures (T > 150 °C), such as selective catalytic reduction (SCR), iron oxide coatings (Fe_2O_3), fly ash surfaces, or aluminum oxide (Al_2O_3) [24,25]. At sufficiently high temperatures (>250 °C), TiO_2 also pro- vides a catalytic surface without UV irradiation [26]. TiO_2 can scavenge mercury passively through oxide-coated windows while utilizing solar UV radiation [27]. Such a system may even function under relatively high mercury concentrations.

In this laboratory, we have previously studied various kinetic, thermochemical and mechanisms of mercury in gaseous and aqua- tic phases [28–31]. We have also studied heterogeneous oxidative surfaces for instance, oleic acid oxidation by ozone over thin water films via attenuated total reflectance Fourier transform infrared spectroscopy [32]. In the present study, we compared with literature sources the mechanisms and kinetics of mercury capture over irradiated titanium dioxide. Previous studies used significantly lower mercury concentrations (1–10 ppb) than our experiments. Consequently we have investigated the exhaustibility of TiO_2 over repeated collections of mercury oxide. We demonstrate that TiO_2 could be employed as an efficient means to reduce mercury concentrations in gas streams, even at very high (1–2 ppm) elemental mercury concentrations. We also attempted to resolve whether high and low levels of water vapour inhibit or promote mercury surface oxidation.

2. Method

2.1. TiO_2 coating procedure

TiO_2 coating procedure was followed from Fernandez et al. [33]. Thirteen milliliter of Ti(IV) isopropoxide was added to 87 mL of isopropyl alcohol and stirred together in a small beaker. Solution depicted slight yellow colour likely due to oxidation with water vapour. A circular disk of quartz (4.8 cm diameter, 0.32 cm thick) was lowered edge-wise into the solution. The disk was slowly re- moved from solution over 10–15 s and left to oxidize from moisture in ambient air for ca., 3 min. Disk was dipped in solution twice more for a total of three coats. Quartz disk was then heated to 400 °C in an oven for 2 h. Opaque white coating was observed on disk. TiO_2 surface was washed progressively with nitric acid, 18.2 MX Milli-Q water, and HPLC-grade acetone. TiO_2 coating was also removed from one side of disk. Disk was weighed (TiO_2 mass = 1.9 ± 0.1 mg), and density was given as $\rho_{TiO_2} = 3.8 g/cm^3$[17]. Approximate average thickness, h, of TiO_2 coating was estimated as h = TiO_2 mass/(disk area × TiO_2 density) = 0.3 μm. The calculated thickness compares reasonably with Fernandez et al. [33], who obtained a thickness of 0.2 μm (no error reported).

The apparent rate constant of the catalytic photo-oxidation of $Hg^0(g)$ over TiO_2 reaction was determined by measuring the relative loss of [$Hg^0(g)$] via electron impact (EI) ionization mass spectrometry (HP-5973). We performed the separation of $Hg^0(g)$ from other constituents on a gas chromatograph (HP-6890) equipped with a 30 m 0.25 mm i.d. 1.0 mm o.d. crossed-linked phenyl- methyl–siloxane column (HP5-MS). The column was operated at a constant flow (1.5 mL min^{-1}) of ultra pure helium. During chromatographic runs, we typically kept the GC oven isothermal at 45 °C (0 °C = 273.15 K) for 1 min and increased the temperature at a rate of 25 °C min^{-1} from 45 to 80 °C.

The quartz disk was inserted into the flask, a volume of 950 mL. Except for quartz window, the flask was made of borosilicate glass. Mercury and toluene samples were added to the reaction flask via vacuum line and gas syringe, respectively, and measured for consistency via GC/MS. The reaction flask was coated with MTO-Halo- carbon Wax (Supelco) to inactive surface adsorption of reactants, products, or reaction intermediates to lead undesired side and secondary reactions due to non-TiO_2 surfaces. The effect of wax coating has been previously studied by our group [30].

Radiation was produced from a 100 W Hg lamp housed in a casing (Oriel, 6281 and 60076) attached with a rear reflector. The radiation power was measured with a UVA detector (PMA2110, Solar Light Company, Inc. 370 nm peak response). At 15 cm, radiation power was approximately 66 ± 5 mW/cm^2. Temperature of reaction was based on ambient conditions, T = 24 ± 2 °C, P = 770 ± 5 torr. Estimation of errors was determined based on daily temperature, pressure, and UV emission fluctuations.

Scanning electron microscopy (SEM) and electron dispersive X-ray spectroscopy (EDS) were performed before and after mercury surface deposition on TiO_2 film. What appeared as mercury deposits were visible in SEM as lightly coloured (white) deposits. The HgO deposits appeared concentrated in particular regions. Focusing the X-ray beam on these regions showed the presence of mercury (Fig. 2). No visible or chemical signs of mercury were found before irradiation and grey areas in Fig. 2 had a minimum of mercury. Switching to a topographical display (Fig. 3), the deposits were apparently localized on the summits of TiO_2 growths.

2.2. Materials

An initial concentration of 1–2 ppm Hg (1 ppm = 2.46 10^{13} molecules cm^{-3} at T = 25 °C, P = 760 torr) was used in experiments. Titanium (IV) isopropoxide (97%) was obtained from Aldrich. HPLC-grade isopropyl alcohol (99.7%), HPLC-grade acetone (99.5%), and 68–70% Nitric acid were all used as delivered from ACP Chemicals. HPLC-grade toluene (99.8%) was obtained from Fisher chemicals.

Standard deviations between repeated experimental trails were performed when available. For individual datum, errors were estimated from equipment uncertainties.

3. Results and discussion

It is reported that the heterogeneous rate of reaction is proportional to the available surface area and light intensity [15,34,35]

$$r = k\theta I^{\alpha} \tag{3}$$

where k is the deposition rate constant [units: molecule min^{-1} cm^{-2} $(mW/cm^2)^{-a}$], I is the UV light intensity, and h the fraction of available surface. We have assumed a constant intensity of UV light, so that I has been incorporated implicitly into k, i.e. $k^0 kI^a$ (prime is omitted henceforth). Fluctuations in light sources are therefore an experimental source of error. Further assuming mercury adsorption obeyed the Langmuir–Hinshelwood mechanism

$$\theta = \frac{K_{Hg}[Hg]}{1 + K_{Hg}[Hg]} \tag{4}$$

where K_{Hg} was the Langmuir adsorption constant (units: cm^3/molecule) and [Hg] was the concentration of mercury in the flask, by combining (1) and (2) to form a predictive rate law, we obtained:

$$Rate = -\frac{1}{A_{TiO_2}}\frac{d\mathrm{Hg}}{dt} = k\frac{K_{\mathrm{Hg}}[\mathrm{Hg}]}{1 + K_{\mathrm{Hg}}[\mathrm{Hg}]} \tag{5}$$

$$-\frac{d[\mathrm{Hg}]}{dt} = \frac{A_{TiO_2}k}{V_f}\frac{K_{\mathrm{Hg}}[\mathrm{Hg}]}{1 + K_{\mathrm{Hg}}[\mathrm{Hg}]} \tag{5′}$$

A_{TiO_2} was the area of the TiO_2 disk and V_f was the volume of the flask. The left hand side of the equation, V_f was divided by absolute mercury losses, converting them into mercury losses per unit volume.

Integrating over $[0,t]$ and $[[Hg]_0, [Hg]_t]$, we obtained:

$$[Hg]_0 - [Hg]_t + \frac{1}{K_{Hg}} \ln\left(\frac{[Hg]_0}{[Hg]_t}\right) = \frac{k}{V_f} A_{TiO_2} t_{irrad.} \quad (6)$$

where $t_{irrad.}$ is the irradiation time of the TiO_2 plate. Re-arranging,

$$\frac{\ln([Hg]_0/[Hg]_t)}{[Hg]_0 - [Hg]_t} = \frac{A_{TiO_2} k K_{Hg}}{V_f} \times \frac{t_{irrad.}}{[Hg]_0 - [Hg]_t} - K_{Hg} \quad (6')$$

Plotting $y = \frac{\ln([Hg]_0/[Hg]_t)}{[Hg]_0 - [Hg]_t}$ versus $x = \frac{t_{irrad.}}{[Hg]_0 - [Hg]_t}$ yielded an intercept $-K_{Hg}$ and slope AkK_{Hg}/V_f. The intercept hence must be negative to have physical meaning.

The associated uncertainties are

$$\delta y = \frac{\delta[Hg]_t}{([Hg]_0 - [Hg]_t)^2} \{(\ln([Hg]_0/[Hg]_t) - [Hg]_0/[Hg]_t + 1)^2 + (\ln([Hg]_t/[Hg]_0) - [Hg]_t/[Hg]_0 + 1)^2\}^{1/2}$$

$$\delta x = \frac{t_{irrad.}}{[Hg]_0 - [Hg]_t} \left\{ \left(\frac{\delta t_{irrad.}}{t_{irrad.}}\right)^2 + 2\left(\frac{\delta[Hg]_t}{[Hg]_0 - [Hg]_t}\right)^2 \right\}^{1/2}$$

assuming d[Hg]$_t$ ¼ d[Hg]$_0$ ~ 50 ppb; dt ~ 0:04 min.

assuming $\delta[Hg]_t = \delta[Hg]_0$ ~50 ppb; δt~0.04 min.

The values k and K_{Hg} can be solved knowing the area of the TiO_2 plate and the flask volume. Typical plot of mercury loss via Hg lamp is shown in Fig. 1. The decay was initially proportional to irradiation time; afterward the decay logarithmically decreased with time. Rate constants are shown in Table 1.

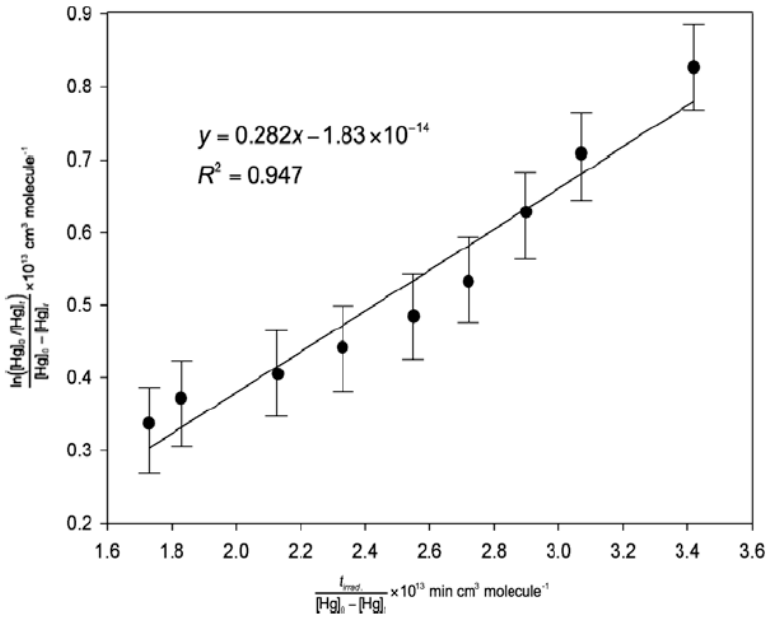

Fig. 1. Plotting Eq. (4), monitoring mercury ($Hg^0(g)$) losses from UVA-irradiated TiO_2. While possible concomitant reactions are occurring to explain this graph, the LH mechanism is the best approximation we currently have.

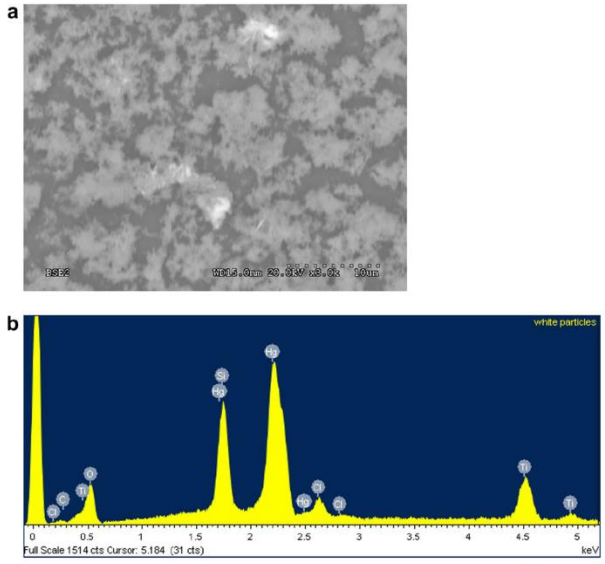

Fig. 2. (a) SEM image (3000× magnification) of TiO_2 displaying white patches, confirmed to be HgO via EDX. (b) EDX of marked area shows presence of TiO, and Hg.

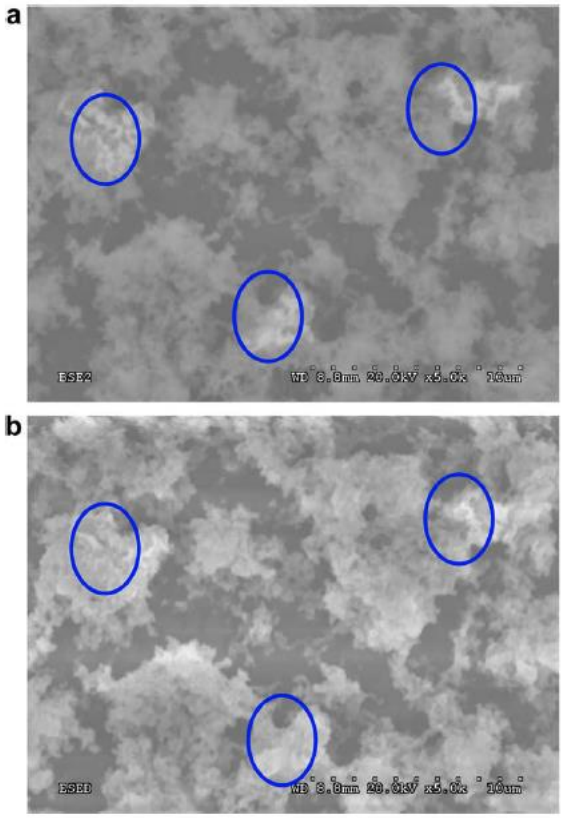

Fig. 3. (a) TiO_2 image using back-scattered electron (BSE). BSE indicates there are at least two distinct compounds. Deposits are circled. (b) Imaging using environmental secondary electron detector (ESED). ESED topographically shows HgO is located on peaks of TiO_2.

3.1. Evaluation of Langmuir–Hinshelwood mechanism

The LH mechanism assumes the reactants (mercury and water) first adsorb onto the surface and then react on the same surface. Mechanistically, mercury appears that it must adsorb onto the sur- face of the TiO_2 film before reacting; experiments performed with- out the TiO_2 catalyst in the presence of UV light showed no signs of mercury oxidation. The adsorption of water is quite strong according to previous studies [36]. Finally, the HgO(s) deposit clearly formed onto the surface to such an extent that it became visible after several hours of continuous UV exposure.

The Eley–Rideal mechanism [5] is an alternative explanation, whereby water adsorbs to the surface but mercury reacts while remaining in the gas phase. This mechanism would imply $Hg^0(g)$ concentrations are linear with reaction rates. Experimentally, the linearity of *logarithmic* plots at lower mercury concentrations (<1 ppm) versus time indicates the LH mechanism is more valid for our experiments.

Table 1
Langmuir adsorption constant K_{Hg} and rate constant k with comparison of affecting parameters.

Ref.	T (°C)	UV power (mW/cm^2)	[Hg] (ppb)	Air flow rate (L/min)	Detection	K_{Hg} (cm^3/molecule)	k (molecule min^{-1} cm^{-2})
A	23–26	44–70	1000–2000	0	MS–EI	$5.1 \pm 2.4 \times 10^{-14}$	$7.4 \pm 2.5 \times 10^{14}$
B	75–80	1.85	0.2–0.3	1	CVAA	13×10^{-14}	3.8×10^{14}
C	43	4	10–80	2	ZAAS–HFM	156×10^{-14}	$(2.4 \times 10^{-4}) \times 10^{14}$

(A) This work, UV source: Oriel 100 W Hg lamp (UVA and B emission), UVA detector: SolarLight PMA2110, MS–EI: HP 5973 Mass Spectrometer Electron Ionization (B) Rodriguez et al. [15], UV source: XX-40 Spectronics 80 W (UVA emission), CVAA: cold vapour atomic adsorption (Shimadzu UV-1201S Spectrometer), UV detector unknown. (C) Li and Wu [22,23], UV source unknown, UV detector: UVX radiometer with UVX-36 sensor probe (335–380 nm range), ZAAS–HFM: Zeeman atomic absorption spectrometry using high frequency modulated light polarization (OhioLumex Co. RA-915+).

3.2. *Comparison of calculated K_{Hg} and k to literature*

To our knowledge, no direct measurement of K_{Hg} for photo-activated titanium dioxide surface values has been obtained in the literature, and our current value represents the first estimation. We compared with the model of Rodriguez et al. [15] by deriving an interpretive value for K_{Hg}. Rodriguez's rate-loss for mercury predicted for trace water vapour conditions was given as:

$$\frac{-d[Hg]}{dt} = \frac{1}{2}\frac{ba[Hg]}{(1 + c[Hg])} \tag{7}$$

In our experiments where low water vapour concentrations were used (RH 6 1%), Eq. (5) seemed analogous to our own Eq. (3). Comparatively, adsorption constant K_{Hg} in Eq. (3) corresponded to constant 'c', hence

$$K_{Hg} = c \tag{8}$$

Rate constant 'k' was also equivalent coefficient in Eqs. (3) and (5):

$$k = \frac{V_f}{A_{TiO_2}}\frac{ab}{2c} \tag{9}$$

Converted values were shown in Table 1.

The reported K_{Hg} and k values were found to be within the same range of magnitudes as Rodriguez et al. [15]. Li and Wu [22], how- ever, clearly show dissimilar values; their calculated K_{Hg} was 30 times larger while k was 10^{-5} times smaller. The agreement between Rodriguez's data is likely explained by both experiments having used a pure TiO_2 surface rather than a SiO_2–TiO_2 composite. It is noteworthy that our operating temperature was lower while UV light intensities were much higher than Rodriguez et al., the light intensity effect was studied in the following section.

3.3. *Sources of uncertainties*

The percentage errors for K_{Hg} and k were 47% and 34%, respectively. The error ranges are large, likely due to several factors: (A) UV intensity varies with distance/angle of lamp while TiO_2 films also varied in thickness depending on XY-surface position. (B) Surface TiO_2 temperatures may vary from the measured bulk temperature of the flask. (C) Cleanliness of the TiO_2 plate. (D) The presence of any volatile organic compounds (VOCs). TiO_2 is known to oxidize most VOCs, thus competing with Hg deposition. We did not, however, see any MS signals for VOCs except acetone, whose concentration remained unchanged during experiments.

3.4. *Light intensity*

Light intensity has been shown to affect the Langmuir adsorption constant [37]. We measured a broad range of UVA intensities from the lamp, ranging from 44 to 70 mW cm^{-2} depending on the angle and position of the detector. Hence our Oriel lamp was not a homogenous light source. An 'average' intensity near the centre of the beam is given here as 60 mW cm^{-2}. According to Fujishima et al., given this high intensity range of light, our experiments may actually lie in a mass transport-controlled region of space [34]. Hence UV light may have saturated the reaction rate and lamp fluc- tuations could be of small concern.

3.5. *TiO_2 disk characteristics and surface area*

The optimal surface density for a TiO_2 coating has been sug- gested to be 0.23 mg cm^{-2} [38]. Thick films attenuate UV light be- fore reaching the surface while too-thin films do not fully absorb the UV light. Our films were approximately 0.1–0.2 mg/cm^2 corre- sponding well with this 'optimal' value. We assumed the surface area of the quartz disk would represent, at least, the perpendicular area exposed to the UV light, about 18 cm^2. Scanning electron microscopy (SEM) analysis of TiO_2 plates (Fig. 2) indicated uniform coverage over the surface, with uneven thicknesses throughout the deposition. The surface area in our sample was unknown. Back- scattering images show the areas with HgO accumulation, whereas environmental secondary electron detector (ESED) imaging show a topographical image of TiO_2 with sharp peaks and valleys. Using energy dispersive X-ray (EDX) spectroscopy, Ti, O, and Hg signals were observed.

3.6. *Saturated HgO deposits*

Experiments in which a mercury-saturated humid air stream passed over the TiO_2 film created a dark deposit of HgO. We reached the saturation point of HgO, whereby reactivity of the TiO_2 film ceased. The deposit was visible to the naked eye, however the exact thickness is not known.

3.7. *Mechanism of Hg_{ads} oxidation (with and without presence of water)*

In our experiment, hydroxyl radicals was expected to oxidize the adsorbed mercury, Hg_{ads} into HgO (the intermediate HgOH is unstable) [15] on the TiO_2 surface. We considered the possibility that ozone was generated in our reaction chamber, however sev- eral trails were performed on gaseous mercury without the pres- ence of TiO_2 and no reaction took place.

There has been a dispute as to whether water vapour promotes or inhibits mercury oxidation [15,22,23]. Mechanistically, water molecules are thought to be required in generating OH radicals that oxidize mercury. The rate-limiting concentration of water needed for mercury oxidation is unclear. In experiments where we heated the TiO_2 plate (to 120 °C) prior to chamber assembly and flushing

the flask with dry air, the rate-loss of mercury remained constant. Hence we found it unnecessary to add water deliberately to incur reactivity. We estimate between 5 and 20 ppm of water might be present in these 'dry' air experiments. Over a rutile TiO_2 surface, water adsorbs to a significant degree; degassing can be detected above 300 °C under vacuum as Hydroxyl groups are chemisorbed to the surface [36]. In more humid conditions (up to 100% relative humidity at 25 °C), mercury oxida- tion again remained the same. Excessive water did not present a strong influence over reactivity, yet is required in only minute concentrations.

Although some studies indicate that the presence of moisture is not necessarily essential to keep up the photocatalytic process [39], further studies under controlled dry conditions and over the larger range of water and other potential co-pollutants concentrations such as NO_x (=NO + NO_2), SO_x (=SO_2 + SO_3), volatile organic compounds are recommended as such species are known to inhibit mercury adsorption [27,40,41].

4. Conclusions

Titanium dioxide is an attractive method of oxidizing gaseous mercury using potentially safe, low-cost procedures. TiO_2 has a high Hg^0 uptake capacity, is relatively cheap (1.09–1.19 USD/lb [42]), and environmentally benign (e.g. currently used in tooth- paste and suntan lotion). The power cost of running continuous UV lights remains a problem [40]. Ultra Violet LEDs will save on en- ergy, hence total cost, provided the LEDs themselves are inexpen- sive and sufficiently [43]. TiO_2 doped for a shift in visible light conversion will may allow for the use of sunlight radiation in mer- cury capture [27].

We have measured the overall rate constant k and Langmuir adsorption constant K_{Hg} in dry and humid air at room temperature and pressure. Measured values were comparable to Rodriguez [15] but clearly distinct from Wu and Li [22,23]. We have addressed the impact of water vapor on the adsorption-oxidation efficiency of mercury on TiO_2 surfaces and did not observe any major impedi- ments on Hg oxidation process even at higher relative humidities. As for the utility of TiO_2 nanoparticles for Hg^0 removal in a coal plant, it is known SO_2 will inhibit TiO_2 surface reactions [19] but this is true of other methods as well [5]. Rising temperatures, espe- cially above 100 °C, might inhibit oxidation [19,35], which in turn emphasizes on the potential of TiO_2 nanoparticles for industrial usage, particularly as the downstream and upstream cooling are part of the existing industrial pollution industries. Life-cycle anal- ysis of photo-activated titanium oxides methods for removal of mercury and the secondary reactions in the environment should be studied to assure its benign nature in the environment. Addi- tives such as gold nanoparticles [44–46] to titanium dioxide coat- ings should be explored for enhanced mercury adsorption properties.

References

[1] F. Bakir et al., Science 181 (1973) 230.
[2] E.G. Pacyna, J.M. Pacyna, Water Air Soil Pollut. 137 (2002) 149.
[3] J. Luna-Camara, Electric Power Monthly Energy Information Administration, 2009.
[4] H. Yi, J. Hao, X. Tang, Energy Policy 35 (2007) 907.
[5] A.A. Presto, E.J. Granite, Environ. Sci. Technol. 40 (2006) 5601.
[6] C.H. Lamborg, W.F. Fitzgerald, J. O'Donnell, T. Torgersen, Geochim. Cosmochim. Acta 66 (2002) 1105.
[7] F.M.M. Morel, A.M.L. Kraepiel, M. Amyot, Ann. Rev. Ecol. Syst. 29 (1998) 543.
[8] U. Diebold, Surf. Sci. Rep. 48 (2003) 53.
[9] A.L. Linsebigler, G. Lu, J.T. Yates, Chem. Rev. 95 (1995) 735.
[10] K. Rajeshwar, J. Ibanez, Environmental Electrochemistry, Academic Press Inc., San Diego, 1996.
[11] R.I. Bickley, T. Gonzalez-Carreno, J.S. Lees, R.J.D. Tilley, L. Palmisano, J. Solid State Chem. 92 (1991) 178.
[12] U. Kaluza, H.P. Boehm, J. Catal. 22 (1971) 347.
[13] C.Y. Wu, T.G. Lee, G. Tyree, E. Arar, P. Biswas, Environ. Eng. Sci. 15 (1998) 137.
[14] T.G. Lee, J.E. Hyun, Chemosphere 62 (2006) 26.
[15] S. Rodríguez, C. Almquist, T.G. Lee, M. Furuuchi, E. Hedrick, P. Biswas, J. Air Waste Manag. Assoc. 54 (2004) 149.
[16] X. Feng, J.Y. Lu, D.C. Grègoire, Y. Hao, C.M. Banic, W.H. Schroeder, Anal. Bioanal. Chem. 380 (2004) 683.
[17] R.C. Weast, CRC Handbook of Chemistry and Physics, CRC Press, Boca Raton, FL, 2007.
[18] J.D. Noel, P. Biswas, D.E. Giammar, J. Air Waste Manage. Assoc. 57 (2007) 856.
[19] T.G. Lee, P. Biswas, E. Hedrick, Am. Inst. Chem. Engrs. 47 (2001) 954.
[20] E. Pitoniak, C.-Y. Wu, D.W. Mazyck, K.W. Powers, W. Sigmund, Environ. Sci. Technol. 39 (2005) 1269.
[21] M.R. Prairie, L.R. Evans, B.M. Stange, S.L. Martinez, Environ. Sci. Technol. 27 (1993) 1776.
[22] Y. Li, P. Murphy, C.-Y. Wu, Fuel Process. Technol. 89 (2008) 567.
[23] Y. Li, C.-Y. Wu, Environ. Eng. Sci. 24 (2007) 3.
[24] C.S. Turchi, Novel Process for Removal and Recovery of Vapor-Phase Mercury, ADA Technologies, Inc., Littleton, CO, 2000, p. 57.
[25] E.J. Granite, H.W. Pennline, Ind. Eng. Chem. Res. 41 (2002) 5470.
[26] K.C. Galbreath, C.J. Zygarlicke, Fuel Process. Technol. 65–66 (2000) 289.
[27] E.J. Granite, W.P. King, D.C. Stanko, H.W. Pennline, Main Group Chem. 7 (2008) 227.
[28] B. Pal, P.A. Ariya, Environ. Sci. Technol. 38 (2004) 5555.
[29] B. Pal, P.A. Ariya, Phys. Chem. Chem. Phys. 6 (2004) 572.
[30] G. Snider, F. Raofie, P.A. Ariya, Phys. Chem. Chem. Phys. 10 (2008) 5616.
[31] P.A. Ariya, K. Peterson, G. Snider, M. Amyot, in: N. Pirrone, R.P. Mason (Eds.), Mercury Fate and Transport in the Global Atmosphere, Springer US, New York, 2009, p. 459.
[32] H.-M. Hung, P. Ariya, J. Phys. Chem. A 111 (2007) 620.
[33] A. Fernandez et al., Appl. Catal. B 7 (1995) 49.
[34] A. Fujishima, T.N. Rao, D.A. Tryk, J. Photochem. Photobiol. C 1 (2000) 1.
[35] T.G. Lee, P. Biswas, E. Hedrick, Ind. Eng. Chem. Res. 43 (2004) 1411.
[36] F. Rouquerol, J. Rouquerol, K. Sing, Adsorption by Powders and Porous Solids, Academic Press, London, 1999, p. 287.
[37] Y. Xu, C.H. Langford, J. Photochem. Photobiol. A 133 (2000) 67.
[38] V. Keller, P. Bernhardt, F. Garin, J. Catal. 215 (2003) 129.
[39] S. Hager, R. Bauer, G. Kudielka, Chemosphere 41 (2000) 1219.
[40] C.R. McLarnon, E.J. Granite, H.W. Pennline, Fuel Process. Technol. 87 (2005) 85.
[41] A.A. Presto, E.J. Granite, Environ. Sci. Technol. 41 (2007) 6579.
[42] L. Terry, Titanium Dioxide (TiO_2) Prices and Pricing Information, ICIS, 2009.

[43] A. Fujishima, X. Zhang, C. R. Chim. 9 (2006) 750.
[44] M. Daté, Y. Ichihashi, T. Yamashita, A. Chiorino, F. Boccuzzi, M. Haruta, Catal. Today 72 (2002) 89.
[45] I.M. Arabatzis, T. Stergiopoulos, D. Andreeva, S. Kitova, S.G. Neophytides, P. Falaras, J. Catal. 220 (2003) 127.
[46] A.A. Presto, E.J. Granite, Platinum Met. Rev. 52 (2008) 144.